Asian Journal of Chemistry; Vol. 33, No. 12 (2021), 3025-3030

ASIAN JOURNAL OF CHEMISTRY

https://doi.org/10.14233/ajchem.2021.23467

Theoretical Molecular Properties Prediction, Docking and Antimicrobial Studies on Anisidine-Isatin Schiff Bases

G.K. AYYADURAI[1,*], R. JAYAPRAKASH[2] and S. RATHIKA[3]

[1]Department of Chemistry, Sri Sairam Engineering College, Sai Leo Nagar, West Tambaram, Chennai-600044, India
[2]Department of Chemistry, School of Arts and Science, Aarupadai Veedu Institute of Technology Campus, Vinayaka Mission's Research Foundation (DU), Paiyanur, Chennai-603104, India
[3]Department of Chemistry, Sri Sairam Institute of Technology, Sai Leo Nagar, West Tambaram, Chennai-600044, India

*Corresponding author: E-mail: ayyaduraisairam@gmail.com

Received: 8 August 2021; *Accepted*: 20 September 2021; *Published online*: 6 December 2021; AJC-20594

The continuous intake of a specific antibiotic for diseases is continuously reducing the immunity of the human in course of time, which includes Covid-19 treatment. Recent research on Schiff bases shows the promising biological activities and good antibacterial results. In this study, three Schiff bases with lactam ring using isatin and three different anisidines in presence of acetic acid were synthesized and characterized. Drug likeness was examined using Molsoft and docking against the target proteins such as 5J6R, 3L9L, 5HVY, covid main protease and 3ZBO proteins for drug suitability. The experimental antibacterial activity against Gram-positive strains like *Staphylococcus aureus*, *Bacillus subtilis* and *Staphylococcus epidermidis*. Among the synthesized compounds, three Schiff bases *ortho* and *meta* substituted compounds exhibited good results when compared to *para* compound, where the methoxyl group position effect was observed.

Keywords: Schiff base, Anisidine, Isatin, Molecular docking, Antimicrobial activity.

INTRODUCTION

In present COVID-19 scenario, new antibacterial, antifungal and immunity boosting synthetic molecules requirement has been increased throughout the world. Synthetic organic compounds with imine functional group are showing various biological applications and have shown significant results in pharmaceutical field [1]. Imine derivatives exhibit good biological results such as anti-inflammatory, analgesic and antimicrobial activities [2]. Schiff bases acted as an execellent donor molecules due to azomethine group (–CH=N-), which is involved in the biological activities [3]. Lactam ring containing an endogenous compound isatin and its derivatives are playing a vital role in medicinal field, which is used as a building molecule to design the pharmacological active molecules [4,5].

Computational chemistry field is used to measure the various theoretical drug related structural parameters to avoid the wastage of the time and chemicals [6-8]. Some of the online tools like Molsoft and molinspiration are providing theoretical QSAR parameters based on the Lipinski five rules [9,10]. In addition to these QSAR softwares, both online and offline docking softwares are adopted to find the ligand or small molecules interaction against the disease causing target proteins theoretically [7-11]. Antibiotic nature of the compounds is examined through the antibacterial studies on using agar broth medium [12]. Based on the above said facts, this article reports the three different Schiff bases from isatin and three anisidines (*ortho*, *meta*, *para*). The derived organic Schiff bases were characterized using UV-Visible, FTIR, ^{1}H NMR and ^{13}C NMR techniques. The theoretical drug related parameters were also calculated using Molsoft online tool. Additionally, the molecules ligand-protein interactions were analyzed using offline CLC drug discovery work bench-4 and online COVID docking server using 5J6R, 3L9L, 5HVY, COVID main protease and 3ZBO proteins. Theoretical outcomes were compared with the experimental antimicrobial activity on selected thick cell wall Gram-positive bacterial strains such as *Bacillus subtilis*, *Staphylococcus aureus* and *Staphylococcus epidermidis*. From the outcomes, the effect of methoxy group position also compared for the future investigations.

EXPERIMENTAL

All the chemicals were purchased from SRL chemicals, India and AR grade solvents were used after purification. The UV-visible spectra of the Schiff bases were recorded using LS25-UV Perkin-Elmer. FT-IR of the Schiff bases was recorded as KBr pellet using JASCO FTIR-6300. Both ^{1}H & ^{13}C magnetic resonance spectra of the Schiff bases recorded in Bruker NMR-400 spectrometer in DMSO-d_6. Theoretical QSAR drug parameters were calculated for the Schiff bases using Molsoft online tool. Proteins PDB files of 5J6R, 3L9L, 5HVY, COVID main protease and 3ZBO targets were obtained from RCSB data bank (https://www.rcsb.org/pdb/home/home.do). Online docking conducted using COVID-19 server against corona virus main protease. Similarly, offline docking conducted using CLC drug discovery work bench-3 software at glutamine active site. Antimicrobial activities were tested on Gram-positive strains such as *Staphylococcus aureus* MTCC 1430, *Bacillus subtilis* and *Staphylococcus epidermidis*. All the strains were purchased from American type culture collections. This work adopted agar well diffusion method to measure the antimicrobial activity. The results were compared with the standard antibiotics like secondary amide group containing gentamycin and lactam ring containing amoxicillin, respectively.

Synthesis of isatin-anisidine condensed Schiff bases (1a-c): Isatin (10 mmol, 1.47 g) was treated with 50 mL ethanol along with 0.7 mL acetic acid in 250 mL three-necked round bottom flask and stirred for 15 min at room temperature. After stirring, 1.23 g of *o*-anisidine in 25 mL of ethanol was added dropwise over a period of 10 min and again stirred for 5 min at room temperature (**Scheme-I**). The reaction mixture was refluxed for 2 h [13,14]. The reaction progress was monitored by TLC using 60:40 ethyl acetate-hexane and small drop of acetic acid. The product isolated after the filtration and recrystallized from 95:5 ethanol and water. Same procedure was followed for the synthesis of *meta* and *para* anisidine Schiff bases (**1b, 1c**).

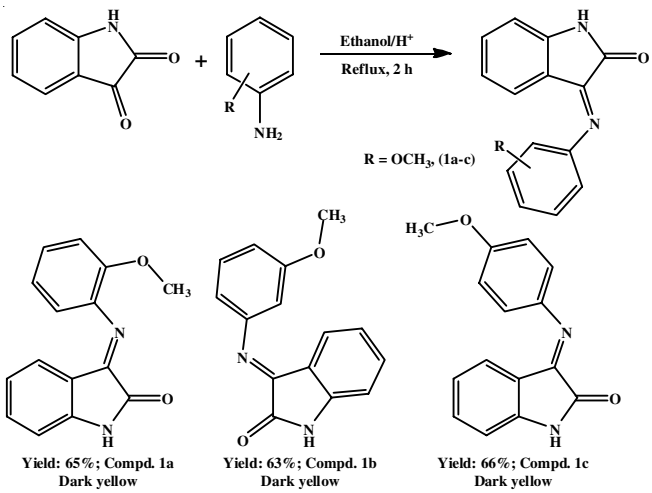

Scheme-I: Synthesis of isatin-anisidine Schiff bases (**1a-c**)

3-[(2-Methoxyphenyl)imino]-1,3-dihydro-2*H*-indol-2-one (1a): Yield 65%; m.p.: 280-285 ºC; ^{1}H NMR (500 MHz, DMSO-d_6): δ 10.53 (s, 1H), 8.12 (dd, *J* = 6.9, 1.2 Hz, 1H), 7.56-7.49 (m, 2H), 7.47 (dd, *J* = 7.6, 2.2 Hz, 1H), 7.36 (qd, *J* = 7.4, 1.7 Hz, 2H), 7.19 (dd, *J* = 7.3, 1.4 Hz, 1H), 7.13 (td, *J* = 7.2, 1.2 Hz, 1H), 3.88 (s, 3H). ^{13}C NMR (125 MHz, DMSO-d_6): δ 161.99, 154.04, 143.30, 142.70, 141.23, 127.79, 126.89, 123.82, 123.58, 123.42, 122.89, 120.81, 111.86, 111.20, 56.04.

3-[(3-Methoxyphenyl)imino]-1,3-dihydro-2*H*-indol-2-one (1b): Yield 63%; m.p.: 278 ºC; ^{1}H NMR (500 MHz, DMSO-d_6): δ 10.55 (s, 1H), 8.13 (dd, *J* = 6.9, 1.2 Hz, 1H), 7.53 (td, *J* = 7.2, 1.0 Hz, 1H), 7.47 (dd, *J* = 7.7, 2.3 Hz, 1H), 7.36 (td, *J* = 7.0, 2.0 Hz, 1H), 7.31-7.22 (m, 2H), 6.94-6.87 (m, 1H), 6.78 (t, *J* = 2.0 Hz, 1H), 3.82 (s, 3H). ^{13}C NMR (125 MHz, DMSO-d_6): δ 161.83, 160.56, 152.17, 147.50, 142.75, 130.52, 23.78, 122.89, 122.80, 120.81, 119.58, 111.86, 109.88, 107.56, 55.18.

(3-[(4-Methoxyphenyl)imino]-1,3-dihydro-2*H*-indol-2-one (1c): Yield 66%; m.p.: 309-317 ºC; ^{1}H NMR (500 MHz, DMSO-d_6): δ 10.57 (s, 1H), 8.13 (dd, *J* = 6.8, 1.2 Hz, 1H), 7.53 (td, *J* = 7.2, 1.0 Hz, 1H), 7.47 (dd, *J* = 7.7, 2.3 Hz, 1H), 7.39-7.31 (m, 3H), 7.09-7.03 (m, 2H), 3.78 (s, 3H). ^{13}C NMR (125 MHz, DMSO-d_6): δ 161.81, 158.01, 147.18, 146.11, 142.75, 124.33, 123.78, 122.89, 122.82, 120.81, 114.30, 111.86, 55.35.

Antibacterial activity: Based on the encouraged results of docking, the experimental antibacterial activity was conducted using 50 µg/mL of standard and two fold quantity of compounds (100 µg/mL) (**1a-c**) by agar well-diffusion method against selected Gram-positive bacteria. As per the reported method [15,16], agar well diffusion method was conducted against the selected pathogens. After the incubation period, inhibition zones of the compounds was measured in millimeter including standard antibiotics such as gentamycin and amoxicillin.

Pharmacokinetic properties in drug design (1a-c): The compounds were drawn in the online molsoft tool and their drug related physico-chemical properties were predicted for the further investigations.

RESULTS AND DISCUSSION

Three different Schiff base molecules of heterocyclic isatin for the Gram-positive bacterial inhibition study were successfully synthesized. In addition, anisidine was selected for the synthesis due to non-polar property of the methoxy group, which may increases the solubility of the isatin derivative after the imine conversion. Solubility property and drug actions are inter-related properties. Also, the non-polar methoxy group position effect was investigated for the further chemical structure modifications. Almost all the molecules have shown slight difference in physical parameters like colour and melting point.

UV-visible studies: The electronic spectra of the synthesized compounds OANIS (**1a**), MANIS (**1b**) and PANIS (**1c**) was recorded in DMSO solvent (Fig. 1). The UV absorption spectra of the synthesized compounds (**1a-c**) exhibited the similar kinds of the peaks with the small deviation in intensity and the wavelength. Schiff bases have shown weak bands between 280 nm and 350 nm for π→π* of imine functional group (–CH=N-), which is due to the chromophore effect. In addition, n→π* transition of imine function exposed the peak between 400 nm and 475 nm (**1a**, **1b, 1c**) with different inten-

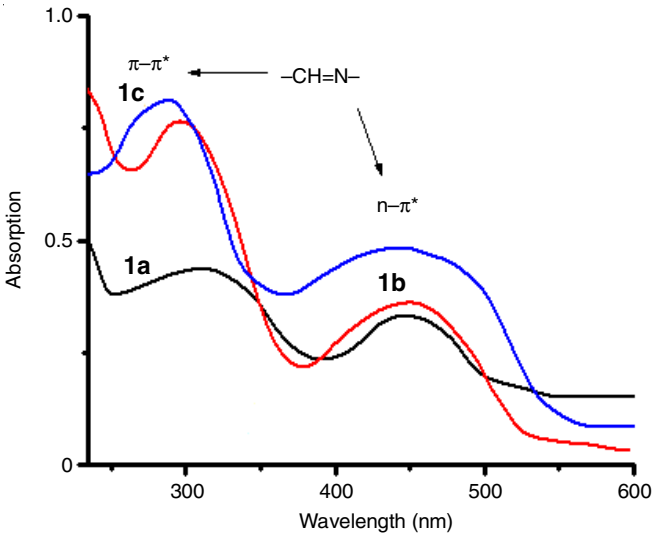

Fig. 1. Absorption spectra of isatin-anisidine Schiff bases (**1a-c**)

sities based on the substituent position. As per the theoretical principle, methoxy group position at *ortho* (7 nm), *meta* (7 nm) and *para* (25 nm) differences were observed in UV spectra and the values are slightly differed due to charge transfer acceptor of methoxy group [17,18].

FT-IR studies: The vibrational spectra of the synthesized compounds were recorded by KBr pellet method. In 3700-3650 cm^{-1} region, the peaks may be due to lactam –C=O group. Similarly, the peaks were observed at 3250-3208 cm^{-1} for lactam N-H, 3000-2970 cm^{-1} peaks for -C-H-Ar and based on the substituents imine group intensity and positions were observed between 1610 and 1594 cm^{-1}. The outcome values are almost concurrence with the reported values [19]. The peaks intensities and the methoxy group's effect on vibrational peaks were observed at 2900 to 2835 cm^{-1}. Similarly, in the vibrational spectra frequency variation observed at 1400 to 1200 cm^{-1} based on the methoxy group position. This may be due to the intramolecular hydrogen bond in *ortho* derivative and it is decreasing gradually from *meta* to *para* derivatives. In *para*-molecule, intermolecular hydrogen bond may be formed.

NMR studies: ^{1}H NMR confirmed the heterocyclic lactam ring proton (–NH) peaks at 10.53 ppm to 10.57 ppm. Aromatic ring protons were observed between 7 ppm and 8.2 ppm, which is coincidence with the reported values [20]. Methoxy group protons were observed at near 3.8 ppm and confirmed the synthesized molecules. Similarly, the ^{13}C NMR peaks were observed for the molecules and almost coincidence with the reported values. Hetero-ring carbons and imine carbons exhibited at higher ppm between 150 and 165 ppm.

Lipinski's rules of five and other criteria: The calculated values were compared with the Lipinski rules of five such as molecular weight less than 500, log P < 5, HBD (hydrogen bond donors) < 5, HBA (hydrogen bond acceptors) < 10 and Molar refractivity value must be in between 40 and 130 [21]. The molsoft outcomes are presented in Table-1. Predicted values fullfilled the Lipinski drug likeness properties. Also, the derived molecules drug likeness increases from -0.68 to -0.25 which is nearing 1 based on the position of the methoxy group. When compare to *ortho* group *para* group drug likeness increased may be due to absence of the steric hinderence, hydrogen bonding, respectively.

After the computational theoretical concurrence of the molecular properties, the molecules were carried for the docking studies against target proteins. Blood brain barrier values are existing in between the limit and the molecules are having good permeability in human body [22]. Molecular polar surface area and the volume are showing the good permeability nature and the values are compared with the standard drug amoxicillin. When compared to the standard, the values are some how differed due to the molecularity and functional groups carboxylic acid group, free amine. While removing the hydroxyl functional group, the drug likeness value decreased from 1.34 to 1.04. Similarly, the druglikeness values were also calculated by removing some functional groups of amoxicillin structure such as –COOH (0.62), $-NH_2$ (0.32) and sulphur ring (0.12). Atlast druglikeness calculated for lactam ring and it exposed -1.60 which is more than the synthesized compounds (**1a-c**).

Docking study: Due to the supporting theoretical drug likeness values, the compounds **1a, 1b** and **1c** were carried for the further ligand-protein interaction studies against human disease causing proteins. Initially, Chemdraw sketched structures were imported to CLC drug discovery workbench-3 software as mol structure format. Then, the target proteins were imported to the same software as PDB format. The imported molecules and proteins were docked individually at the selected binding

TABLE-1
PHYSICO-CHEMICAL PROPERTIES OF COMPOUNDS **1a-c**

Parameters	Compound **1a**	Compound **1b**	Compound **1c**	Amoxicillin
Molecular formula	$C_{15}H_{12}N_2O_2$	$C_{15}H_{12}N_2O_2$	$C_{15}H_{12}N_2O_2$	$C_{16}H_{19}N_3O_5S$
Molecular weight	252.09	252.09	252.09	365.10
Number of HBA	3	3	3	7
Number of HBD	1	1	1	5
MolLog P	2.39	2.67	2.41	-0.66
MolLog S	-2.98	-3.52	-3.02	-1.61
MolPSA	39.15 A^2	39.76 A^2	39.76 A^2	108.61 A^2
MolVol	256.83 A^3	256.62 A^3	256.55 A^3	361.41 A^3
pKa/Acidic group	0.45/15.54	0.55/15.42	1.25/15.42	6.55/3.66
BBB score	4.64	4.64	4.64	2.58
Number of stereo centers	0	0	0	4
Drug likeness	-0.68	-0.61	-0.25	1.34

sites of target proteins such as 5J6R (Glu273 of chain A-human papillomavirus 59), 3L9L (Glu121-transferase/transferase inhibitor), 5HVY (Glu99-CDK8 human) and 3ZBO (Glu220-*Bacillus cereus* heat-like replication DNA glycosylases). The interactions were investigated for the further experimental antimicrobial activity on Gram-positive bacterial strains. Glutamine is an important α-amino acid, which is involved in the biosynthesis of proteins [23-25]. Hence, the docking carried at that site. The offline docking outcomes have presented in Table-2. Similarly, the molecules mol structure were subjected to COVID server for online docking against COVID main protease to measure the efficacy of the molecules even it may be a simple molecules when compare to the developed countries COVID-19 vaccines [26]. The values are compared with the reported docking scores of the commercial drug molecules [27]. The docking scores of molecules against the COVID main protease are included in Table-2. Some of the docked poses are shown in Fig. 2. The docking 3D outcomes were modified to 2D structures using bio-discovery visual studio software. Some of the converted 2D images are presented in Fig. 3. The 2D structures are showing good binding ability of the both imine and lactam ring active sites on target proteins binding sites. Additionally, these compounds mol structures were submitted in COVID-19 online server to dock against COVID-19 main protease one by one [28]. The outcomes of each compounds are presented in Table-2.

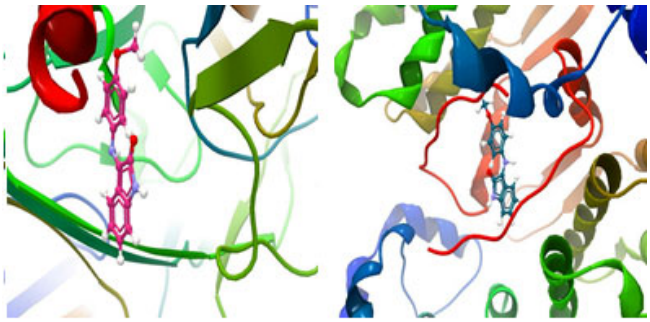

1a-3L9L 1a-5HVY

Fig. 2. Some of the offline docking poses of compounds **1a-c**

Further, the molecular docking carried for amoxicillin antibiotic is used as an antibiotic for COVID-19 pandemic. The docking results of standard amoxicillin and the derivatives were compared for the further antibacterial studies. The highest score docked poses are presented in Fig. 4. The resultant scores are exposing nearby values. Amoxicillin showed higher interaction score against 5J6R and COVID main protease. But, the observed difference against corona virus protein exists between 0.60 kcal mol^{-1} and 0.90 kcal mol^{-1}. Similarly,

TABLE-2
DOCKING SCORES OF COMPOUNDS **1a-c** SCHIFF BASES

Compd.	Docking scores in kcal mol^{-1}				
	5J6R	3L9L	5HVY	Covid Main Protease	3ZBO
1a	-24.14	-45.60	-54.37	-7.10 (ID: 202107211910064337)	-39.21
1b	-21.52	-43.78	-51.64	-6.70 (ID: 202107211911103733)	-31.20
1c	-22.68	-40.12	-52.06	-6.80 (ID: 202107211911433451)	-46.77
Amoxicillin	-38.40	-40.32	-46.03	-7.70 (ID: 202108050131368577)	-42.01

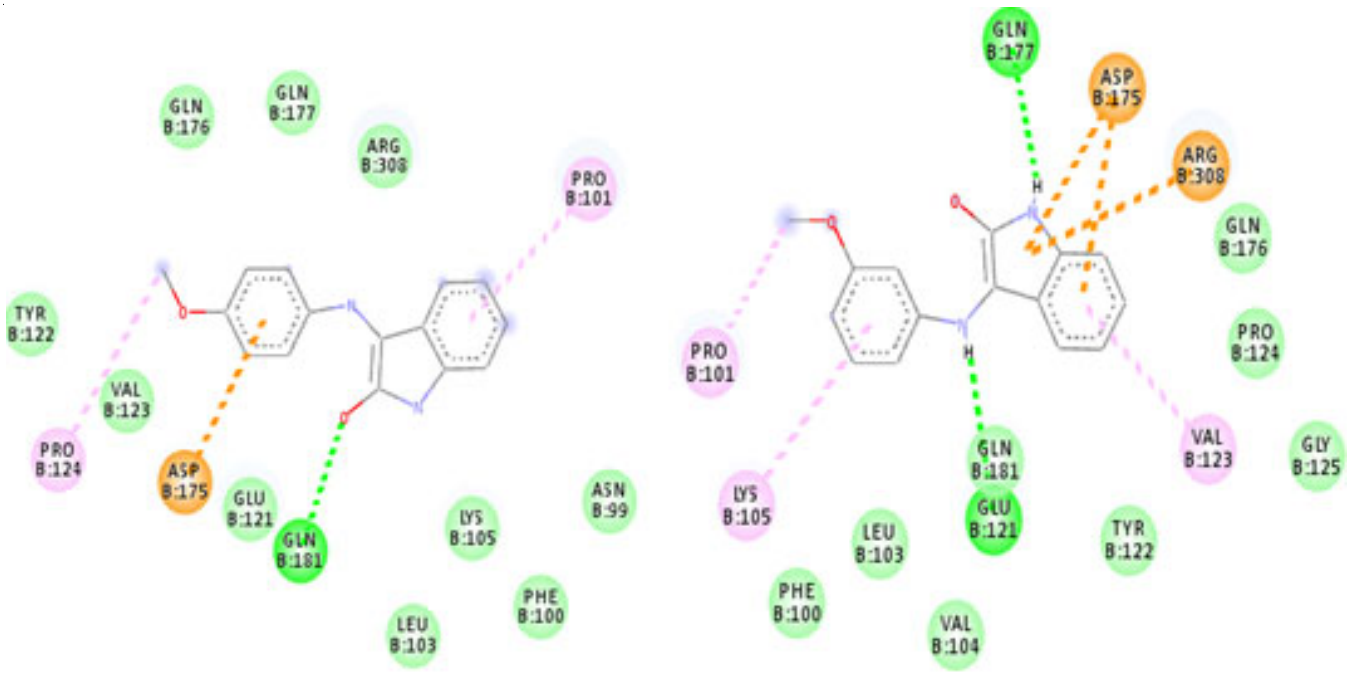

(a) 1c-5HVY (b) 1a-5HVY

Fig. 3. 2D images of the docking poses of compounds **1c** and **1b** against 5HVY

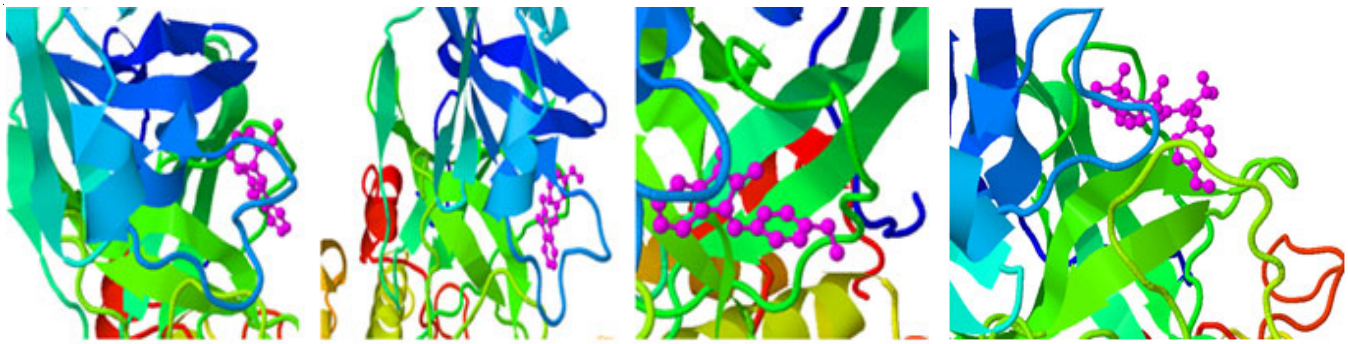

Fig. 4. Some of the online docking poses of compounds **1a-c**

standard amoxicillin showed the difference between -14.26 kcal mol^{-1} and 16.88 kcal mol^{-1} against 5J6R papillomavirus. The combination of hydrogen bond, electrostatic free energy, torsional free energy, internal energy and van der Waals energy in terms of binding energy docking score. The docking scores of the derived comp-ounds and the standard amoxicillin exposed the good comple-xing tendency with the targets which is controlling the growth of the proteins.

Antimicrobial activity: The molecules were carried for the antimicrobial activity against Gram-positive bacteria. Except the *para* molecules, *ortho* and *meta* parameters show good inhibition against the three selected bacterial strains. The synthesized molecules **1a, 1b** have shown good inhibition zones between 14 mm and 16 mm when compared with the standards, the molecules showed the good inhibition than gentamycin and less or equal to standard amoxicillin (Table-3). Also, these *ortho* and *meta* compounds have shown good inhibition results when compare to *para* derivative. The results of **1c** against *Staphylococcus aureus* almost coincidence with the reported results [17]. Synthesized isatin Schiff bases showed good inhibition results due to β-lactam ring with donor imine group except *para* compound [29]. The present work observed the good results against *Staphylococcus epidermidis*. The reason is attributed to due to the formation of the complex between the cell wall of *Staphylococcus epidermidis* teichoic acid based polymer product and thereby may be control the further protein formation.

TABLE-3
ANTIBACTERIAL ACTIVITY RESULTS OF COMPOUNDS **1a-c** AND THE STANDARD ANTIBIOTICS

Compd.	Zone of inhibition (mm)		
	Staphylococcus epidermidis	*Staphylococcus aureus*	*Bacillus subtilis*
1a	14 ± 0.30	14 ± 0.02	14 ± 0.04
1b	16 ± 0.29	16 ± 0.31	12 ± 0.11
1c	–	–	4 ± 0.11
Amoxicillin	18 ± 0.22	12 ± 0.02	12 ± 0.06
Gentamicin	12 ± 0.25	10 ± 0.02	–
DMSO	–	–	–

Conclusion

From the theoretical and experimental results, this work understand the effect of methoxy group substituent in drug propertis and experimental results. Methoxy group is non polar charge transfer accepting functional chromophore, which acts as an important role in the drug properties. *Ortho*-position and *meta*-position molecules are having good complexing ability when compare to *para*-position. Hence, *ortho* (**1a**) and *meta* (**1b**) position exposed good antimicrobial activity against the Gram-positive bacteria. In addition, these molecules will be carried for the further improvements by changing the substituent or by converting the functional group.

CONFLICT OF INTEREST

The authors declare that there is no conflict of interests regarding the publication of this article.

REFERENCES

1. A. Kajal, S. Bala, S. Kamboj, N. Sharma and V. Saini, *J. Catal.*, **2013**, 893512 (2013); https://doi.org/10.1155/2013/893512
2. K. Mounika, A. Pragathi and C. Gyanakumari, *J. Sci. Res.*, **2**, 513 (2010); https://doi.org/10.3329/jsr.v2i3.4899
3. K. Mohanan, R. Aswathy, L.P. Nitha, N.E. Mathews and B.S. Kumari, *J. Rare Earths*, **32**, 379 (2014); https://doi.org/10.1016/S1002-0721(14)60081-8
4. E. Bulatov, R. Sayarova, R. Mingaleeva, R. Miftakhova, M. Gomzikova, Y. Ignatyev, A. Petukhov, P. Davidovich, A. Rizvanov and N.A. Barlev, *Cell Death Discov.*, **4**, 103 (2018); https://doi.org/10.1038/s41420-018-0120-z
5. R.P. Chinnasamy, R. Sundararajan and S. Govindaraj, *J. Adv. Pharm. Technol. Res.*, **1**, 342 (2010); https://doi.org/10.4103%2F0110-5558.72428
6. R. Jayaprakash, S.K. Sha, S. Hemalatha and D. Easwaramoorthy, *Int. J. Chemtech Res.*, **9**, 48 (2016).
7. R. Jayaprakash, S.K. Sha, S. Hemalatha and D. Easwaramoorthy, *Asian J. Pharm. Clin. Res.*, **9**, 203 (2016); https://doi.org/10.22159/ajpcr.2016.v9s3.14664
8. S.K. Sha, R. Jayaprakash, S. Hemalatha and D. Easwaramoorthy, *Asian J. Pharm. Clin. Res.*, **11**, 368 (2018); https://doi.org/10.22159/ajpcr.2018.v11i7.25664
9. M.A. Bakht, M.S. Yar, S.G. Abdel-Hamid, S.I. Al Qasoumi and A. Samad, *Eur. J. Med. Chem.*, **45**, 5862 (2010); https://doi.org/10.1016/j.ejmech.2010.07.069
10. I.Z. Benet, C.M. Hosey, O. Ursu and T.I. Oprea, *Adv. Drug Deliv. Rev.*, **101**, 89 (2016); https://doi.org/10.1016/j.addr.2016.05.007
11. S.Y. Ebrahimipour, I. Sheikhshoaie, J. Castro, M. Dušek, Z. Tohidiyan, V. Eigner and M. Khaleghi, *RSC Adv.*, **5**, 95104 (2015); https://doi.org/10.1039/C5RA17524K

12. R. Singh, K. Sharma and R.V. Singh, *J. Sulfur Chem.*, **31**, 61 (2010); https://doi.org/10.1080/17415990903173529
13. K.D. Thomas, A.V. Adhikari, I.H. Chowdhury, T. Sandeep, R. Mahmood, B. Bhattacharya and E. Sumesh, *Eur. J. Med. Chem.*, **46**, 4834 (2011); https://doi.org/10.1016/j.ejmech.2011.07.049
14. J. Azizian, M.K. Mohammadi, O. Firuzi, N. Razzaghi-asl and R. Miri, *Med. Chem. Res.*, **21**, 3730 (2012); https://doi.org/10.1007/s00044-011-9896-6
15. R. Bhatnagar, J. Pandey and D. Panhekar, *Asian J. Chem.*, **32**, 2731 (2020); https://doi.org/10.14233/ajchem.2020.22823
16. F. Hakim and S.R. Salfidoer, *Asian J. Chem.*, **33**, 1757 (2021); https://doi.org/10.14233/ajchem.2021.23226
17. D.R. Brkic, A.R. Bozic, A.D. Marinkovic, M.K. Milcic, N.Z. Prlainovic, F.H. Assaleh, I.N. Cvijetic, J.B. Nikolic and S.Z. Drmanic, *Spectrochim. Acta A Mol. Biomol. Spectrosc.*, **196**, 16 (2018); https://doi.org/10.1016/j.saa.2018.01.080
18. O.S. Oguntoye, A.A. Hamid, G.S. Iloka, S.O. Bodede, S.O. Owalude and A.C. Tella, *J. Appl. Sci. Environ. Manag.*, **20**, 653 (2016); https://doi.org/10.4314/jasem.v20i3.20
19. M. Enamullah, M. Al-moktadir Zaman, M.M. Bindu, M.K. Islam and M.A. Islam, *J. Mol. Struct.*, **1201**, 127207 (2020); https://doi.org/10.1016/j.molstruc.2019.127207
20. D.P. da Costa, A.C. Castro, G.A. Silva and C.G. Lima-Junior, F.P. de Andrade Júnior, E. de Oliveira Lima, B.G. Vaz and L.C. da Silva, *J. Heterocycl. Chem.*, **58**, 766 (2020); https://doi.org/10.1002/jhet.4213
21. C.A. Lipinski, *J. Pharmacol. Toxicol. Methods*, **44**, 235 (2000); https://doi.org/10.1016/S1056-8719(00)00107-6
22. M. Gupta, H.J. Lee, C.J. Barden and D.F. Weaver, *J. Med. Chem.*, **62**, 9824 (2019); https://doi.org/10.1021/acs.jmedchem.9b01220
23. Q. Zeng, J.G. Allen, M.P. Bourbeau, X. Wang, G. Yao, S. Tadesse, J.T. Rider, C.C. Yuan, F.-T. Hong, M.R. Lee, S. Zhang, J.A. Lofgren, D.J. Freeman, S. Yang, C. Li, E. Tominey, X. Huang, D. Hoffman, H.K. Yamane, C. Fotsch, C. Dominguez, R. Hungate and X. Zhang, *Bioorg. Med. Chem. Lett.*, **20**, 1559 (2010); https://doi.org/10.1016/j.bmcl.2010.01.067
24. P. Bergeron, M.F.T. Koehler, E.M. Blackwood, K. Bowman, K. Clark, R. Firestein, J.R. Kiefer, K. Maskos, M.L. McCleland, S. Ramaswamy, L. Orren, L. Salphati, S. Schmidt, E.V. Schneider, J. Wu and M. Beresini, *ACS Med. Chem. Lett.*, **7**, 59 (2016); https://doi.org/10.1021/acsmedchemlett.6b00044
25. K.P. Rakesh, H.K. Kumara, B.J. Ullas, J. Shivakumara and D. Channe Gowda, *Bioorg. Chem.*, **90**, 103093 (2019); https://doi.org/10.1016/j.bioorg.2019.103093
26. E.M. Marinho, J. Batista de Andrade Neto, J. Silva, C. Rocha da Silva, B.C. Cavalcanti, E.S. Marinho and H.V. Nobre Júnior, *Microb. Pathog.*, **148**, 104365 (2020); https://doi.org/10.1016/j.micpath.2020.104365
27. S. Khaerunnisa, H. Kurniawan, R. Awaluddin, S. Suhartati and S. Soetjipto, *Preprints*, 2020030226 (2020); https://doi.org/10.20944/preprints202003.0226.v1
28. R. Kong, G. Yang, R. Xue, M. Liu, F. Wang, J. Hu, X. Guo and S. Chang, *Bioinformatics*, **36**, 5109 (2020); https://doi.org/10.1093/bioinformatics/btaa645
29. H. Guo, *Eur. J. Med. Chem.*, **164**, 678 (2019); https://doi.org/10.1016/j.ejmech.2018.12.017